Taylor & Francis
Taylor & Francis Group

Automatika

Journal for Control, Measurement, Electronics, Computing and Communications

ISSN: 0005-1144 (Print) 1848-3380 (Online) Journal homepage: https://www.tandfonline.com/loi/taut20

Local time-varying topology identification of network with unknown parameters based on adaptive synchronization

Hai-Peng Ren, Kun Tian & Ren Zhou

To cite this article: Hai-Peng Ren, Kun Tian & Ren Zhou (2018) Local time-varying topology identification of network with unknown parameters based on adaptive synchronization, Automatika, 59:3-4, 391-399, DOI: 10.1080/00051144.2018.1552473

To link to this article: https://doi.org/10.1080/00051144.2018.1552473

Published online: 05 Dec 2018.

AUTOMATIKA
2018, VOL. 59, NOS. 3–4, 391–399
https://doi.org/10.1080/00051144.2018.1552473

REGULAR PAPER

OPEN ACCESS Check for updates

Local time-varying topology identification of network with unknown parameters based on adaptive synchronization

Hai-Peng Ren, Kun Tian and Ren Zhou

Shaanxi Key Laboratory of Complex System Control and Intelligent Information Processing, Xi'an University of Technology, Xi'an, People's Republic of China

ABSTRACT

The network with some or all of characteristics including self-organization, self-similarity, attractor, small world and scale-free is referred to as a complex network. A complex network might demonstrate various uncertainties, such as the unknown node kinetics and the unknown network topology. The network topology identification using the observing output data of the network is a crucial step for complex network analysis, which is of great importance to understand the networks' properties and regulate network. In this paper, the output variable is used to drive the response network to identify partial time-varying topology of the drive network with unknown parameters. The synchronization between the response network and drive network and the successful identification are guaranteed by the Lyapunov stability theorem. The feasibility of the proposed method is demonstrated using two examples.

Ovo je primjer sažetka. Ovo je primjer sažetka. Ovo je primjer sažetka. Ovo je primjer sažetka. Ovo je primjer sažetka. Ovo je primjer sažetka. Ovo je primjer sažetka. Ovo je primjer sažetka. Ovo je primjer sažetka. Ovo je primjer sažetka. Ovo je primjer sažetka. Ovo je primjer sažetka. Ovo je primjer sažetka.

KEYWORDS

Complex network; partial topology identification; synchronization; unknown parameters

KLJUČNE RIJEČI

Croatian; translation; keywords

1. Introduction

From electric power networks, traffic networks to communication networks and network of friends, people live in a wide variety of networks. There are a lot of researches focusing on how the dynamic behavior of the network is affected by the topology and the characteristics of the complex network. On the contrary, there are few works on finding the network topology using the output of the network. For example, the regulatory relationship between nodes (topology) is extremely complicated in the gene regulatory network, which is important for protein synthesis and disease treatment as discussed elsewhere [1]. Parameters identification has also wide applications [2]. Hence, it is of great importance for both theoretical research and applications to identify the network topology using the observed node output. The existing topology identification methods can be divided into several classes including synchronization-based methods, compressive sensing theory-based methods, etc.

Synchronization-based topology identification methods are the most commonly used methods. Yu et al. [3] and Zhou and Lu [4] used the synchronization-based methods to identify the network topology. Liu et al. [5] and Xu et al. [6] considered the network with unknown dynamical parameters of the node and identified the network topology and dynamical parameters simultaneously, using the same way as that in references [3–4]. Liu et al. [7] obtained better identification result using projection synchronization, and identified the network topology and node dynamical parameters at the same time. Zhang et al. [8] proposed a topology identification method based on generalized outer synchronization, a response network with simple node dynamics was constructed and used for synchronization with the drive network with complex node dynamics, which reduces the complexity of identification. Jiang et al. [9] and Wan et al. [10] used the output variable to drive the response network for identifying the topology without the requirement to measure all state variables of the nodes. Zhou et al. [11] and Wallace et al. [12] transmitted the first state of the node dynamics to the response network to reduce the number of state variables used for synchronization; however, the proposed method needs to measure the specified state in the drive network; meanwhile, a positive-definite function has to be found to satisfy a complex inequality, which restricted the application of the method. Li et al. [13] and Timme [14] identified the phase oscillator network topology by repeating experiments many times based on phase synchronization, which needs a large amount of calculation for large-scale networks. Yang and Wei [15] and Liu et al. [16] introduced the impulse control strategy for network topology identification to

CONTACT Hai-Peng Ren renhaipeng@xaut.edu.cn Shaanxi Key Laboratory of Complex System Control and Intelligent Information Processing, Xi'an University of Technology, 5 South Jinhua Road, Xi'an, Shaanxi 710048, People's Republic of China

save the control energy. Stanković et al. [17] proposed to estimate all system parameters utilizing a stochastic approximation algorithm with the expanding truncation derived from the modified Yule-Walker equations. Chen et al. [18] analysed the influence of the synchronization among the nodes in the drive network on the topology identification procedure and proposed two methods to avoid the drive network synchronization including changing the coupling strength or modifying the output function, which are difficult to do for the practical complex networks. Sun et al. [19] pointed out that the response network could synchronize with the drive network within the time span needed for the drive network from its initial state to the self-synchronization state. Reference [20] used this idea and the optimization method to search response network parameters to achieve synchronization between the drive network and the response network before the drive network itself falls into the synchronization state. Reference [21] used partial states observation and the parameter optimization method to identify the network parameters based on the objective function containing only available states. Reference [22] proposed the chaotic ant swarm algorithm to search (and identify) the parameters of the network. Van den Hof et al. [23] treated the identification of network as a classical closed-loop system identification so that a module or sub-system can be identified. For the networks with sparse connections, Ke [24] proposed a least squares model with ℓ^1 -regularized output and used the weight iterative least squares method to identify the parameters, which is proved to be a very efficient way for the large-scale network using the data with or without noise. Chiuso and Pillonetto [25] proposed a Bayesian approach to identify dynamical network with sparse connection based on the estimation of impulse responses from a finite set of input–output data. Vašak and Perić [26] utilized piecewise affine models to approximate nonlinear systems and to identify system parameters.

The compressive sensing concept was also used for the network topology identification. Hayden et al. [27] proposed the compressing sensing method to reconstruct the sparse connection dynamical network. Wang et al. [28] and Su et al. [29] expanded node nonlinear differential equations into its power series, Li et al. [30] used the Taylor series expansion of the node nonlinear differential equation; then, by using compressive sensing theory, they obtained the network topology. Since this method used the advantage of the compressive sensing algorithm, the more sparse the connection vector, the less observational data required for topology identification.

The difficulties of the complex network topology identification are as follows: (1) time-varying topology: the network topology varies over time due to the reason like the congestion of signal transmission as discussed elsewhere [31]; (2) unknown parameters of the node dynamics; (3) only part of the node states are available for the identification; and (4) when the network size is large, the computational cost of the existing methods increases significantly. For the network with N nodes, there are N^2 topology parameters to be identified, the calculation needed is huge for the large-scale network; however, in some practical situations, only a part of the connection among some important nodes are concerned. Therefore, it is not necessary to identify the whole network topology. The existing methods do not consider all the above factors, e.g. References [3,4,8,10,11,12] cannot handle the unknown parameters in the node dynamics, References [5–7] required that all state variables are measurable, which cannot be used when only partial state variables are available. All methods above considered the time-invariant network topology. In this paper, we proposed a method to identify local time-varying topology of the network with unknown node dynamical parameters using partial available state variables, which involves all the above constraints.

The rest of this paper is arranged as follows: Section 2 gives the problem description; Section 3 gives the proposed method and its stability proof using the Lyapunov method; Section 4 gives simulation results to show the effectiveness of the proposed method and Section 5 gives some conclusions.

2. Problem description

Consider a complex dynamical network consisting of N nodes given by

$$\dot{\boldsymbol{x}}_i = f_i(\boldsymbol{x}_i) + g_i(\boldsymbol{x}_i)\boldsymbol{\alpha}_i + \sum_{j=1}^{N} b_{ij}(t)\boldsymbol{K}y_j, \quad i = 1, 2, \ldots, N, \tag{1}$$

where $\boldsymbol{x}_i = [x_{i1}, x_{i2}, \ldots, x_{in}]^{\mathrm{T}} \in R^n$ is the state vector of node i, $\boldsymbol{\alpha}_i \in R^{m_i}$ is the unknown dynamical parameter vector, $\bar{f}_i = f_i(\boldsymbol{x}_i) + g_i(\boldsymbol{x}_i)\boldsymbol{\alpha}_i$, $f_i(\boldsymbol{x}_i) \in R^n$, $g_i(\boldsymbol{x}_i) \in R^{n\times m_i}$, $\boldsymbol{B}(t) = (b_{ij}(t))_{N\times N} \in R^{N\times N}$ is a topology matrix, if there is a connection between node i and node j, b_{ij} is not zero, otherwise, $b_{ij}$is zero. $\boldsymbol{K} = [k_1, k_2, \ldots, k_n]^{\mathrm{T}}$ is the gain vector, $y_i = \boldsymbol{H}\boldsymbol{x}_i \in R$ is the output of node i, $\boldsymbol{H} = [h_1, h_2, \ldots, h_n]$ is the output coupling vector.

Assumption 2.1: *Suppose that there exists a positive constant L_i satisfying*

$$||\bar{f}_i(\boldsymbol{x}, \boldsymbol{\alpha}_i) - \bar{f}_i(\hat{\boldsymbol{x}}, \boldsymbol{\alpha}_i)|| \le L_i||\boldsymbol{x} - \hat{\boldsymbol{x}}||, \tag{2}$$

where $\boldsymbol{x}$, $\hat{\boldsymbol{x}}$ are time-varying vectors and $||\bullet||$ represents norm.

Assumption 2.2: *$\boldsymbol{K}y_i (i = 1,2, \ldots, N)$ are independent.*

Assumption 2.3: *At any time, the time-varying topology* $|\dot{b}_{ij}(t)| \leq Q$.

Assumption 2.4: *In the output coupling model, the state variables with coupling are observable.*

Assume that the dynamic characteristics of nodes are consistent. In order to identify the unknown parameter $\boldsymbol{\alpha}_i$ and part of unknown topology matrix $\boldsymbol{B}$, we consider another complex dynamical network with a controller $\boldsymbol{u}_{i'}$ as follows:

$$\dot{\hat{\boldsymbol{x}}}_{i'} = f_{i'}(\hat{\boldsymbol{x}}_{i'}) + g_{i'}(\hat{\boldsymbol{x}}_{i'})\hat{\boldsymbol{\alpha}}_{i'} + \boldsymbol{u}_{i'}, \quad i' = 1, 2, \ldots, M, \tag{3}$$

where i' is the concerned node, M is the total number of the concerned nodes, $\hat{\boldsymbol{x}}_{i'} = [\hat{\boldsymbol{x}}_{i'1}, \hat{\boldsymbol{x}}_{i'2}, \ldots, \hat{\boldsymbol{x}}_{i'n}]^{\mathrm{T}} \in R^n$ is the response state vector of the node i' in the considered response network, $\hat{\boldsymbol{\alpha}}_{i'}$ is the estimation of $\boldsymbol{\alpha}_{i'}$ and $\boldsymbol{u}_{i'}$ is the control input vector.

3. Local topology identification method and its stability analysis

In order to identify the parameter $\boldsymbol{\alpha}_{i'}$ and topology matrix $\boldsymbol{B}$, the control laws are proposed as follows:

$$\begin{aligned}
\boldsymbol{u}_{i'}(t) &= -d_{i'}(t)\boldsymbol{I}(\hat{y}_{i'} - y_{i'}) + \sum_{j=1}^{N} \hat{b}_{i'j}(t)\boldsymbol{K}y_j, \\
\dot{d}_{i'}(t) &= \gamma_{i'} e_{y_{i'}}^T \boldsymbol{H}\boldsymbol{I} e_{y_{i'}}, \\
\dot{\hat{b}}_{i'j}(t) &= -e_{y_{i'}}^T \boldsymbol{H}\boldsymbol{K}y_j, \\
\dot{\hat{\boldsymbol{\alpha}}}_{i'} &= -g_{i'}^T(\hat{\boldsymbol{x}}_{i'}(t))\boldsymbol{H}^{\boldsymbol{T}} e_{y_{i'}},
\end{aligned} \tag{4}$$

where $\boldsymbol{I} = [1\ 1 \ldots 1]^{\mathrm{T}} \in R^n$, $\hat{b}_{i'j}(t)$ is the estimation of $b_{i'j}(t)$ and $\gamma_{i'} > 0$ is a constant. We give the following theorem to guarantee the stability of the controller and the convergence of the identification procedure.

Theorem 3.1: *Suppose that Assumptions from 2.1 to 2.4 are satisfied, if there is a sufficiently large positive constant* $d_{i'}^*$ *such that*

$$L_{i'} - d_{i'}^* HI < 0 \quad (i' = 1, 2, \ldots, M), \tag{5}$$

the control law in (4) makes the network (3) synchronize with the corresponding part of network (1), and the local (partial) topology of network (1) can be given by $\hat{b}_{i'j}(t)$.

Proof: . By defining $\boldsymbol{e}_{i'} = \hat{\boldsymbol{x}}_{i'} - \boldsymbol{x}_{i'}$, $\tilde{\boldsymbol{\alpha}}_{i'} = \hat{\boldsymbol{\alpha}}_{i'} - \boldsymbol{\alpha}_{i'}$ and $\tilde{b}_{i'j}(t) = \hat{b}_{i'j}(t) - b_{i'j}(t)$, we have the error dynamics as follows:

$$\begin{aligned}
\dot{\boldsymbol{e}}_{i'} &= \bar{f}_{i'}(\hat{\boldsymbol{x}}_{i'}) - \bar{f}_{i'}(\boldsymbol{x}_{i'}) - \sum_{j=1}^{N} b_{i'j}\boldsymbol{K}y_j + \boldsymbol{u}_{i'} \\
&= \bar{f}_{i'}(\hat{\boldsymbol{x}}_{i'}, \boldsymbol{\alpha}_{i'}) - \bar{f}_{i'}(\boldsymbol{x}_{i'}, \boldsymbol{\alpha}_{i'}) + g_{i'}(\hat{\boldsymbol{x}}_{i'})\tilde{\boldsymbol{\alpha}}_{i'} \\
&\quad - \sum_{j=1}^{N} b_{i'j}\boldsymbol{K}y_j + \boldsymbol{u}_{i'}.
\end{aligned} \tag{6}$$

Choose a Lyapunov function candidate as

$$\begin{aligned}
V = &\frac{1}{2}\sum_{i'=1}^{M} e_{y_{i'}}^T e_{y_{i'}} + \frac{1}{2}\sum_{i'=1}^{M}\sum_{j=1}^{N} \tilde{b}_{i'j}^2 + \frac{1}{2}\sum_{i'=1}^{M} \tilde{\boldsymbol{\alpha}}_{i'}^T \tilde{\boldsymbol{\alpha}}_{i'} \\
&+ \frac{1}{2}\sum_{i'=1}^{M} \frac{1}{\gamma_{i'}}(d_{i'}(t) - d_{i'}^{**})^2,
\end{aligned} \tag{7}$$

where $d_{i'}^{**}$ is a sufficiently large positive constant to be determined. The derivative of V is

$$\begin{aligned}
\dot{V} = &\sum_{i'=1}^{M} e_{y_{i'}}^T \dot{e}_{y_{i'}} + \sum_{i'=1}^{M}\sum_{j=1}^{N} \tilde{b}_{i'j}(\dot{\hat{b}}_{i'j} - \dot{b}_{i'j}) + \sum_{i'=1}^{M} \tilde{\boldsymbol{\alpha}}_{i'}^T \dot{\hat{\boldsymbol{\alpha}}}_{i'} \\
&+ \sum_{i'=1}^{M} \frac{1}{\gamma_{i'}}(d_{i'}(t) - d_{i'}^{**})\dot{d}_{i'}(t) \\
= &\sum_{i'=1}^{M} e_{y_{i'}}^T \boldsymbol{H}[\bar{f}_{i'}(\hat{\boldsymbol{x}}_{i'}, \boldsymbol{\alpha}_{i'}) - \bar{f}_{i'}(\boldsymbol{x}_{i'}, \boldsymbol{\alpha}_{i'}) + g_{i'}(\hat{\boldsymbol{x}}_{i'})\tilde{\boldsymbol{\alpha}}_{i'} \\
&- \sum_{i'=1}^{N} b_{i'j}\boldsymbol{K}y_j + \boldsymbol{u}_{i'}] + \sum_{i'=1}^{M}\sum_{j=1}^{N} \tilde{b}_{i'j}\dot{\hat{b}}_{i'j} + \sum_{i'=1}^{M} \tilde{\boldsymbol{\alpha}}_{i'}^T \dot{\hat{\boldsymbol{\alpha}}}_{i'} \\
&+ \sum_{i'=1}^{M} \frac{1}{\gamma_{i'}}(d_{i'}(t) - d_{i'}^{**})\dot{d}_{i'}(t) - \sum_{i'=1}^{M}\sum_{j=1}^{N} \tilde{b}_{i'j}\dot{b}_{i'j} \\
\leq &\sum_{i'=1}^{M} e_{y_{i'}}^T \boldsymbol{H}L_{i'}\boldsymbol{e}_{i'} - \sum_{i'=1}^{M} d_{i'}^{**} e_{y_{i'}}^T \boldsymbol{H}\boldsymbol{I} e_{y_{i'}} \\
&+ \sum_{i'=1}^{M}\sum_{j=1}^{N} Q|\tilde{b}_{i'j}| \\
\leq &\sum_{i'=1}^{M} (L_{i'} - d_{i'}^* \boldsymbol{H}\boldsymbol{I})||e_{y_{i'}}||^2 \\
= &\boldsymbol{E}_y^T \boldsymbol{P}\boldsymbol{E}_y,
\end{aligned} \tag{8}$$

where $\boldsymbol{E}_y = [e_{y_1}\, e_{y_2} \ldots e_{y_M}]^{\mathrm{T}}$ and $P = \mathrm{diag}\{L_1 - d_1^* \boldsymbol{H}\boldsymbol{I}, L_2 - d_2^* \boldsymbol{H}\boldsymbol{I}, \cdots, L_M - d_M^* \boldsymbol{H}\boldsymbol{I}\}$. $\boldsymbol{P}$ is negative definite for large enough positive constant $d_{i'}^{**}$, such that $\sum_{i=1}^{M} (d_{i'}^{**} - d_{i'}^*) e_{y_{i'}}^T \boldsymbol{H}\boldsymbol{I} e_{y_{i'}} \geq \sum_{i'=1}^{M}\sum_{j=1}^{N} Q|\tilde{b}_{i'j}|$, $L_{i'} - d_{i'}^* \boldsymbol{H}\boldsymbol{I} < 0$. Therefore, the largest invariant set in the set

defined by $\dot{V} = 0$ is

$$\bar{M} = \begin{cases} e_{y_{i'}} = 0, \boldsymbol{e}_{i'} = 0, \tilde{\boldsymbol{\alpha}}_{i'} = 0, \dot{\hat{\boldsymbol{\alpha}}}_{i'} = 0, \dot{\hat{b}}_{i'j} = 0, \\ \sum_{j=1}^{N} (\hat{b}_{i'j}(t) - b_{i'j}(t))\boldsymbol{K} y_j = 0, i' = 1, 2, \ldots, M, \\ j = 1, 2, \ldots, N \end{cases}$$

From Assumption 2.2, we know that given arbitrary initial values, $\lim_{t\to\infty} \hat{b}_{i'j}(t) = b_{i'j}(t)$. ■

4. Numerical simulation results

In order to verify the effectiveness of the proposed method, a 10-node network shown in Figure 1 is used as an example. The node dynamics in the network is given by

$$\begin{aligned} \bar{f}_i(\boldsymbol{x}_i) &= f_i(\boldsymbol{x}_i) + g_i(\boldsymbol{x}_i)\boldsymbol{\alpha}_i \\ &= \begin{pmatrix} 0 \\ -x_{i2} - x_{i1}x_{i3} \\ x_{i1}x_{i2} \end{pmatrix} + \begin{pmatrix} (x_{i2} - x_{i1}) & 0 & 0 \\ 0 & x_{i1} & 0 \\ 0 & 0 & x_{i3} \end{pmatrix} \\ &\quad \begin{pmatrix} \alpha_{i1} \\ \alpha_{i2} \\ \alpha_{i3} \end{pmatrix}, \end{aligned} \tag{9}$$

which is the well-known Lorenz system when $\alpha_{i1} = 10$, $\alpha_{i2} = 28$ and $\alpha_{i3} = -8/3$. The topology matrix $\boldsymbol{B}$ for Figure 1 is given by Equation (10). Assume that the output of the node is the first state variable, i.e. $x_{i,1;}$ therefore, $\boldsymbol{H} = [1\ 0\ 0]$, the dynamical parameters of the nodes are unknown, $\boldsymbol{K} = [1\ 1\ 1]^{\mathrm{T}}$. We consider the connections in the first six nodes.

$$B = \begin{bmatrix} -3 - 0.2\cos(\pi t/100) & 1 + 0.2\cos(\pi t/100) & 1 & 0 & 1 & 0 & 0 & 0 & 0 & 0 \\ 0 & -2 & 1 & 1 & 0 & 0 & 0 & 0 & 0 & 0 \\ 0 & 0 & -2 & 1 & 0 & 1 & 0 & 0 & 0 & 0 \\ 0 & 0 & 0 & -1 & 0 & 1 & 0 & 0 & 0 & 0 \\ 0 & 0 & 1 & 0 & -2 & 1 & 0 & 0 & 0 & 0 \\ 0 & 0 & 0 & 0 & 0 & -1 & 1 & 0 & 0 & 0 \\ 0 & 0 & 0 & 0 & 0 & 0 & -2 & 0 & 1 & 1 \\ 0 & 0 & 0 & 0 & 0 & 0 & 1 & -1 & 0 & 0 \\ 0 & 0 & 0 & 0 & 0 & 0 & 0 & 1 & -1 & 0 \\ 0 & 0 & 0 & 0 & 0 & 0 & 0 & 0 & 1 & -1 \end{bmatrix}_{10\times 10} . \tag{10}$$

The identified constant $\hat{b}_{ij}(t)$ among the first six nodes is displayed in Figure 2(a), where different $\hat{b}_{ij}(t)$ is plotted using a different colour. It might be difficult to discriminate them, but from the blow up steady state plot, we know that the $\hat{b}_{ij}(t)$ approach to their true values after a transient oscillation. The time-varying parameters b_{11} and b_{12} are not given in Figure 2(a), but given in Figure 2(b,c), respectively, where the red solid curve represents the time-varying value of the variable and the blue dotted curve represents the estimated value. The identified connection matrix is given by Equation (11) with $\hat{b}_{11}$ and $\hat{b}_{12}$ replaced with "*".

$$\begin{pmatrix} * & * & 1.012 & -0.002 & 0.996 & 0.006 & 0.001 & -0.001 & -0.004 & -0.006 \\ -7.02e-13 & -2.000 & 1.000 & 1.000 & 2.47e-13 & 9.17e-16 & 5.27e-13 & 2.28e-13 & 2.07e-12 & 2.84e-12 \\ -7.28e-15 & -1.43e-15 & -2.000 & 1.000 & -1.91e-15 & 1.000 & 2.06e-15 & 8.99e-16 & -7.03e-15 & -4.59e-15 \\ 2.72e-14 & -1.12e-13 & -1.77e-14 & -1.000 & -9.91e-14 & 1.000 & -2.63e-14 & 5.50e-14 & 6.87e-14 & -1.90e-14 \\ -2.57e-15 & -6.30e-15 & 1.000 & -1.25e-16 & -2.000 & 1.000 & -2.32e-15 & -1.15e-15 & 4.62e-16 & 3.55e-15 \\ -8.63e-16 & 6.58e-15 & -1.62e-15 & -6.09e-16 & 5.03e-15 & -1.000 & 1.000 & -6.39e-15 & -8.95e-15 & -3.51e-15 \end{pmatrix}_{6\times 10} \tag{11}$$

From Equation (11), we learn that, when we truncate the elements in Equation (11) to the corresponding integer, we get a matrix with the same constant elements as those in Equation (10) except the time-varying elements b_{11} and b_{12}. This validates the identification result very well. From Figure 2(b,c), the blue dotted curve can track the red solid curve after a period of transient state. This indicates that the proposed method can identify the time-varying connection effectively. To further validate the identification result, we define the steady state root mean square error of the identification results and is defined by

$$E = \frac{1}{(k_2 - k_1 + 1)M \cdot N} \sqrt{\sum_{i=1}^{M} \sum_{j=1}^{N} \sum_{k=k_1}^{k_2} (b_{ij}(k) - \hat{b}_{ij}(k))^2},$$

where k_1 is the start time of the steady state and k_2 is the end time of consideration, $b_{ij}(k)$ represents the sampled value of $b_{ij}(t = k\Delta t)$ and Δt is the sampling interval, they are the same for $\hat{b}_{ij}$. E for the identified matrix (11) is calculated as 4.9683×10^{-5}, which is a very small value. Since x_{i1} have been used as the driving signal, we use another state variable x_{i2} of the node to verify the validity of identification results as shown in Figure 3. From Figure 3, we know that after a transient process, the state synchronization error tends to 0, which means the states are synchronized and the dynamics of the node are identified correctly. Other nodes' states can also be checked for the same results.

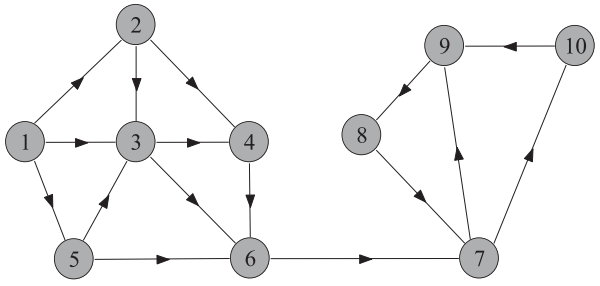

Figure 1. 10-node network topology with node dynamics as the Lorenz system.

A 20-node network shown in Figure 4 is used as another example. The node dynamics in the network is given by

$$\begin{aligned}\bar{f}_i(\boldsymbol{x}_i) &= f_i(\boldsymbol{x}_i) + g_i(\boldsymbol{x}_i)\boldsymbol{\alpha}_i \\ &= \begin{pmatrix} 0 \\ -x_{i1}x_{i3} \\ x_{i1}x_{i2} \end{pmatrix} + \begin{pmatrix} (x_{i2}-x_{i1}) & 0 & 0 \\ 0 & x_{i2} & 0 \\ 0 & 0 & x_{i3} \end{pmatrix} \\ &\quad \begin{pmatrix} \alpha_{i1} \\ \alpha_{i2} \\ \alpha_{i3} \end{pmatrix}, \end{aligned} \tag{12}$$

which is the well-known Lü system when $\alpha_{i1} = 36$, $\alpha_{i2} = 20$, $\alpha_{i3} = -3$. The available output is $x_{i,1}$, i.e. $\boldsymbol{H} = [1\,0\,0]$. The topology matrix $\boldsymbol{B}$ for Figure 4 is given by Equation (13). We are interested in the connections between the first five nodes

$$B = \begin{bmatrix}
-3-0.2\cos(\pi t/500) & 1+0.2\cos(\pi t/500) & 1 & 0 & 1 & 0 & 0 & 0 & 0 & 0 & 0 & 0 & 0 & 0 & 0 & 0 & 0 & 0 & 0 & 0 \\
0 & -2 & 1 & 1 & 0 & 0 & 0 & 0 & 0 & 0 & 0 & 0 & 0 & 0 & 0 & 0 & 0 & 0 & 0 & 0 \\
0 & 0 & -1 & 1 & 0 & 0 & 0 & 0 & 0 & 0 & 0 & 0 & 0 & 0 & 0 & 0 & 0 & 0 & 0 & 0 \\
0 & 0 & 0 & -3 & 0 & 1 & 0 & 1 & 0 & 0 & 0 & 0 & 0 & 0 & 1 & 0 & 0 & 0 & 0 & 0 \\
0 & 0 & 1 & 0 & -2 & 1 & 0 & 0 & 0 & 0 & 0 & 0 & 0 & 0 & 0 & 0 & 0 & 0 & 0 & 0 \\
0 & 0 & 1 & 0 & 0 & -2 & 0 & 0 & 0 & 0 & 0 & 0 & 0 & 0 & 1 & 0 & 0 & 0 & 0 & 0 \\
0 & 0 & 0 & 0 & 0 & 0 & -2 & 0 & 1 & 1 & 0 & 0 & 0 & 0 & 0 & 0 & 0 & 0 & 0 & 0 \\
0 & 0 & 0 & 0 & 0 & 0 & 1 & -2 & 0 & 1 & 0 & 0 & 0 & 0 & 0 & 0 & 0 & 0 & 0 & 0 \\
0 & 0 & 0 & 0 & 0 & 0 & 0 & 1 & -1 & 0 & 0 & 0 & 0 & 0 & 0 & 0 & 0 & 0 & 0 & 0 \\
0 & 0 & 0 & 0 & 0 & 0 & 0 & 0 & 1 & -2 & 1 & 0 & 0 & 0 & 0 & 0 & 0 & 0 & 0 & 0 \\
0 & 0 & 0 & 0 & 0 & 0 & 0 & 0 & 0 & 0 & -1 & 0 & 1 & 0 & 0 & 0 & 0 & 0 & 0 & 0 \\
0 & 0 & 0 & 0 & 0 & 0 & 0 & 0 & 0 & 0 & 1 & -1 & 0 & 0 & 0 & 0 & 0 & 0 & 0 & 0 \\
0 & 0 & 0 & 0 & 0 & 0 & 0 & 0 & 0 & 0 & 0 & 0 & -1 & 1 & 0 & 0 & 0 & 0 & 0 & 0 \\
0 & 0 & 0 & 0 & 0 & 0 & 0 & 0 & 0 & 0 & 1 & 1 & 0 & -2 & 0 & 0 & 0 & 0 & 0 & 0 \\
0 & 0 & 0 & 0 & 0 & 0 & 1 & 0 & 0 & 0 & 0 & 0 & 0 & 0 & -2 & 0 & 0 & 1 & 0 & 0 \\
0 & 0 & 0 & 0 & 0 & 0 & 0 & 0 & 0 & 0 & 0 & 0 & 0 & 0 & 1 & -3 & 1 & 0 & 1 & 0 \\
0 & 0 & 0 & 0 & 0 & 0 & 0 & 0 & 0 & 0 & 0 & 0 & 0 & 0 & 0 & 0 & -1 & 1 & 0 & 0 \\
0 & 0 & 0 & 0 & 0 & 0 & 0 & 0 & 0 & 0 & 0 & 0 & 0 & 0 & 0 & 0 & 0 & -1 & 0 & 1 \\
0 & 0 & 0 & 0 & 0 & 0 & 0 & 0 & 0 & 0 & 0 & 0 & 0 & 0 & 0 & 0 & 1 & 0 & -1 & 0 \\
0 & 0 & 0 & 0 & 0 & 0 & 0 & 0 & 0 & 0 & 0 & 0 & 0 & 0 & 0 & 0 & 0 & 1 & -1 &
\end{bmatrix}_{20\times 20}. \tag{13}$$

The identified constant topology parameters $\hat{b}_{ij}(t)$ in the first five nodes are displayed in Figure 5(a), where the blow up pictures are the steady state values. From Figure 5(a), we know that $\hat{b}_{ij}(t)$ approach to their true values after a transient state. Although one might not be able to discriminate which line corresponds to which b_{ij}, one does see the valid result from the identified matrix given by Equation (14) by truncating the elements to the corresponding integers and comparing them with Equation (13). E calculated for this example is 2.6127×10^{-6}.

Figure 5(b,c) are the identification results of the time-varying topological parameters $\hat{b}_{11}$ and $\hat{b}_{12}$, respectively. The red solid curve in them represents the time-varying value of the variable and the blue dotted curve in them represents the estimated value.

$$\begin{bmatrix}
* & * & 1.002 & 0.001 & 1.005 & -0.004 & -0.002 & -0.003 & -0.005 & -0.005 & 0.003 \\
6.05e-14 & -2.000 & 1.000 & 1.000 & 4.73e-14 & 2.99e-13 & -5.10e-13 & 1.67e-13 & -6.64e-15 & 1.52e-13 & 8.31e-14 \\
9.29e-15 & 2.84e-14 & -1.000 & 1.000 & -4.47-14 & 3.21e-14 & -1.33e-14 & -8.95e-14 & 1.60e-14 & 3.39e-14 & 1.02e-14 \\
6.69e-15 & 6.42e-14 & 7.29e-14 & -3.000 & -9.77e-14 & 1.000 & -7.14e-14 & 1.000 & -6.83e-16 & 5.50e-14 & 3.88e-14 \\
6.98e-14 & 1.34e-13 & 1.000 & 2.74e-14 & -2.000 & 1.000 & -4.02e-14 & -2.12e-13 & -1.42e-13 & 5.41e-14 & 1.86e-13
\end{bmatrix}$$

$$\begin{bmatrix}
-0.008 & 0.002 & 0.006 & -1.50e-04 & -0.003 & -0.004 & -0.011 & -0.001 & -5.97e-04 \\
4.34e-14 & 2.69e-13 & -1.70e-13 & 3.70e-13 & -5.40e-14 & 2.59e-13 & 8.70e-13 & 5.60e-14 & 6.07e-14 \\
7.89e-14 & 1.19e-14 & 2.52e-14 & 8.36e-14 & -5.26e-14 & 1.85e-14 & 1.86e-14 & 1.66e-14 & -8.46e-14 \\
3.96e-14 & 7.77e-15 & -2.40e-14 & 1.000 & -3.74e-15 & 2.25e-14 & 1.58e-14 & 5.58e-14 & -9.42e-14 \\
2.52e-13 & 1.33e-13 & 1.85e-13 & 1.49e-13 & 8.13e-14 & 7.13e-14 & 3.53e-13 & 1.08e-13 & -9.24e-14
\end{bmatrix}_{5\times 20} \tag{14}$$

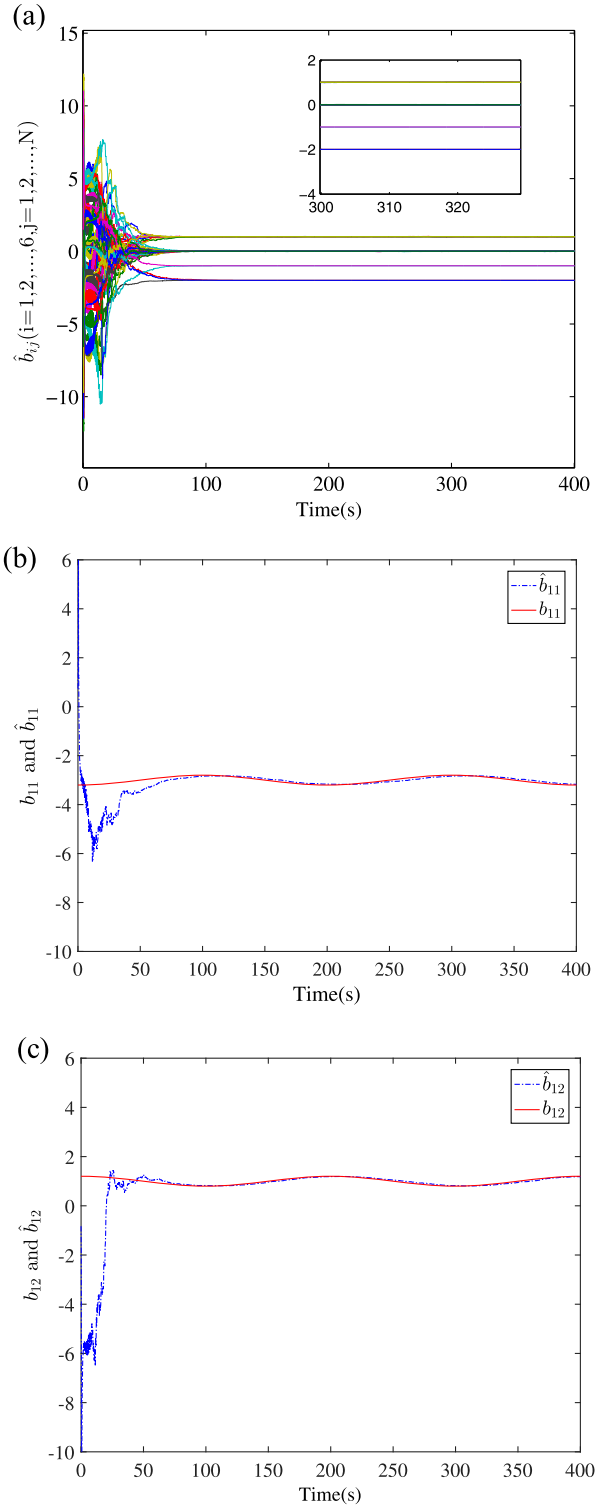

Figure 2. Topology identification results for the 10-node Lorenz network.

From Figure 5(b,c) it can be noted that the blue dotted curve can track the red solid curve after a period of a transient state, which shows the effective identification for the time-varying parameters. We also use another state variable x_{12} to verify the validity of correct dynamics identification, as shown in Figure 6. The results indicate that the identified x_{12} is consistent with that of the driving system.

Reference [10] also considers partial topology observation; however, it cannot deal with the time variant

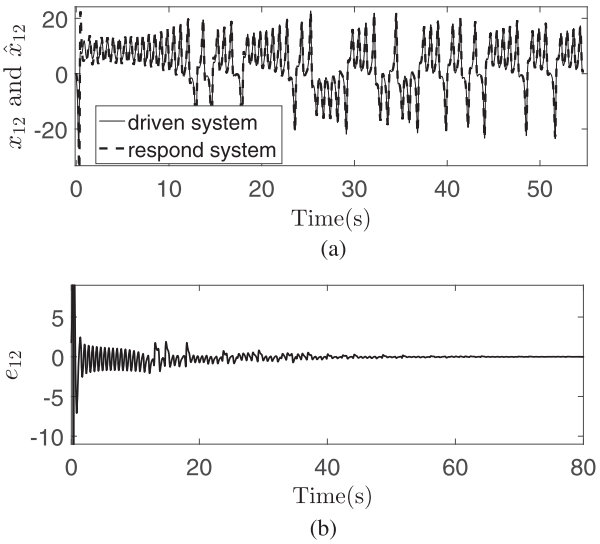

Figure 3. Synchronization error of state x_{12} between the response system and the drive system, subplot (a) is the time sequences of the driving state variable and the corresponding state variable of the response system, subplot (b) is the synchronization error of state x_{12}.

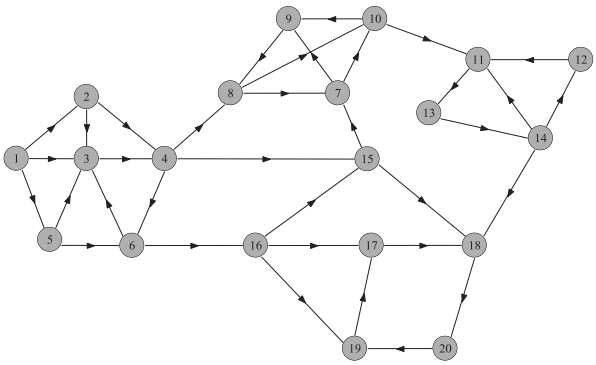

Figure 4. 20-Node network topology with node dynamics as the Lü system.

parameters. To compare our proposed method with the method proposed in [10], we design a test as follows: the dynamical parameter of node 1 in Figure 1, i.e. α_{11} , steps from 10 to 11 at time 200s, the simulation results using our proposed method and the method in [10] are given in Figure 7(a,b), respectively. Comparing Figure 7(a,b), we see that the network topology with variant parameters can be identified correctly using the proposed method, although there exists a transient process. However, the method in [10] fails to identify the parameters after the parameter changes because the time-variant property of the parameters is not considered in the method in [10].

One merit of our proposed method is that it does not need all state variables of the node to accomplish the synchronization with the drive system. However, the selection of the state variable is an important issue. For the same network configuration as shown in Figure 1, if the node output is the second state variable, i.e. $\boldsymbol{H} = [0\ 1\ 0]$, the simulation results given in Figure 8 show that the topology parameters do not converge at all.

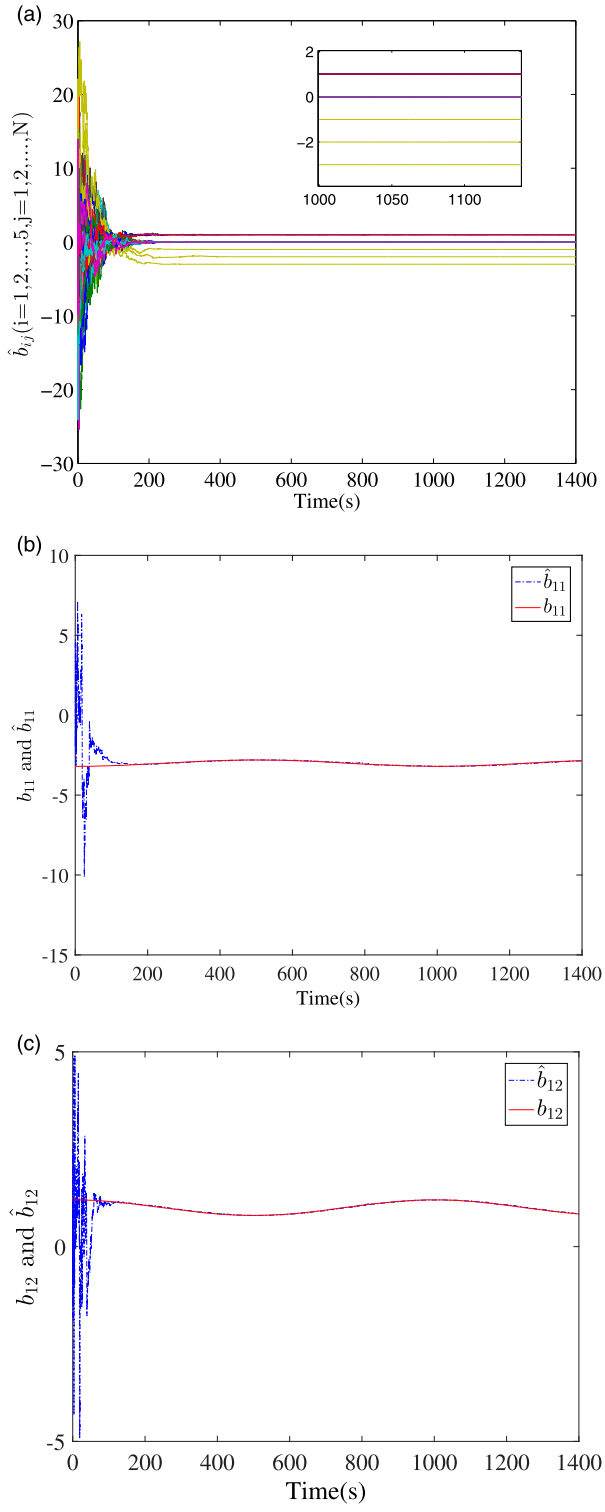

Figure 5. Topology identification results for the 20-node Lü network.

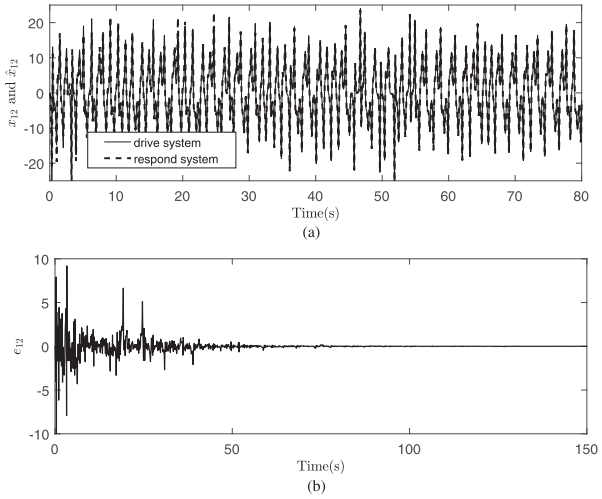

Figure 6. Synchronization error of state x_{12} between the response system and the drive system subplot. (a) Is the time sequences of the driving state variable and the corresponding state variable of the response system and subplot (b) is the synchronization error of state x_{12}.

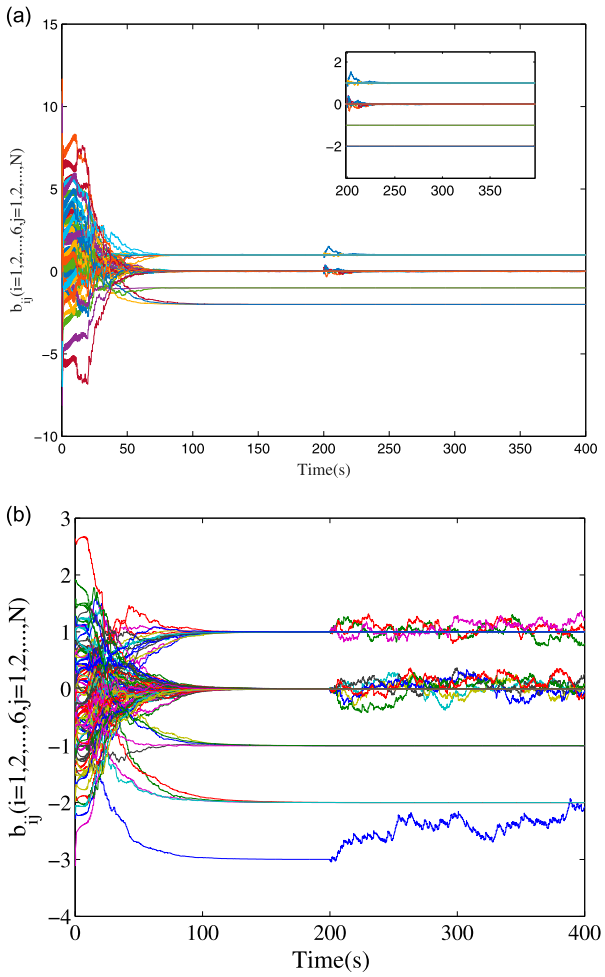

Figure 7. Identified topology of the network with time-variant parameter in Figure 1, when the dynamic parameter α_{11} steps from 10 to 11 at $t = 200$ s.

Similarly, when only the third state of the node is available for identification, it does not work too. The reason for this is that the observability of each state variable in a node dynamics is different. For Lorenz and Lü systems, the first state variable is of the observability as discussed elsewhere [32,33], the other two variables are not. So if the state variable with observability is available for coupling and measurement, the proposed method is effective; otherwise, it fails to identify. From our investigation, the node dynamics being chaotic also helps the identification process.

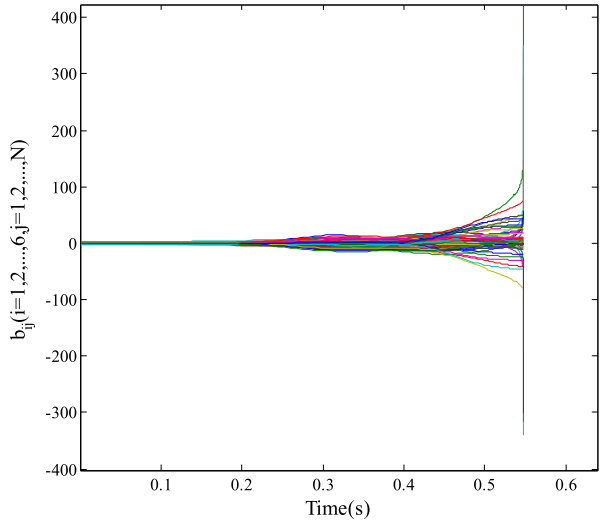

Figure 8. The identified connection parameters when the second state x_{i2} of the nodes in Figure 1 is used as the driving signal.

Discussion 1: Due to the partial nodes being selected to identify, the different groups of nodes will lead to different identification errors. Generally speaking, the more the number of nodes selected, the higher the degree of synchronization, and the less identification error.

Discussion 2: For the same number of nodes selected, the groups with time-variant connection nodes will lead to a larger identification error as compared to the groups without time-variant connection nodes.

Discussion 3: Although there does exist a group of the node with the fixed number of the node having the least identification error among the groups with the same node number. The node selection to be identified depends on the practical requirement, but does not depend on the identification error.

5. Conclusion

In this paper, we propose an adaptive identification method for the topological parameters and the kinetic parameters of the nodes using a synchronization-based way. The stability of the error system is guaranteed by the Lyapunov theory. We use the partial state variables of the network to be identified to drive the response network, which reduces the requirement for all state variables as needed by some existing methods. Our proposed method can identify the partial topological parameters, which reduces the computation cost when the network size is very large. The proposed method can deal with the topological parameter and kinetic parameter variations, which is an obstacle for some existing methods. However, the available state for the specified node dynamics is restricted to the state variables with observability. That means the topology cannot be identified if the drive state variable does not carrying enough dynamical information about the node dynamics.

Disclosure statement

No potential conflict of interest was reported by the authors.

Funding

This work was supported by Key program of Natural Science Foundation of Shaanxi Province [grant number 2016 ZDJC-01].

References

[1] Ren HP, Huang XN, Hao JX. Finding robust adaptation gene regulatory networks using multi-objective genetic algorithm. IEEE/ACM Trans Comput Biol Bioinf. 2016;13(3):571–577.
[2] Čeřovský Z, Lev M. Permanent Magnet Synchronous Machine parameters identification for Load characteristics calculation. Automatika. 2015;56(2):217–225.
[3] Yu D, Righero M, Kocarev L. Estimating topology of networks. Phys Rev Lett. 2006;97(18):188701.
[4] Zhou J, Lu JA. Topology identification of weighted complex dynamical networks. Physica A. 2007;386(1):481–491.
[5] Liu H, Lu JA, Lü JH. Topology identification of an uncertain general complex dynamical network. Proceedings of 2008 IEEE International Symposium on Circuits and Systems(ISCAS); May 2008; Washington, USA; p. 109–112.
[6] Xu JQ, Zhang JX, Tang WS. Parameters and structure identification of complex delayed networks via pinning control. Trans Inst Meas Control. 2012;35(5):619–624.
[7] Liu H, Wang XY, Tan GZ. Structure identification of uncertain complex networks based on anticipatory projective synchronization. Plos One. 2015;10(10):0139804.
[8] Zhang SN, Wu XQ, Lu JA, et al. Recovering structures of complex dynamical networks based on generalized outer synchronization. IEEE Trans. Circuits Systems-I. 2014;61(11):3216–3224.
[9] Jiang FH, Jiang GP, Liu H. Observer-based approach to the topology identification of complex networks. Proceedings of 2010 Chinese control & Decision conference(CCDC); May 2010; Xuzhou, China; p. 938–941 (in Chinese).
[10] Wan YH, Wang SP, Jiang GP. A new state-observer-based approach to the identification of complex dynamical networks. Chin J Electron. 2010;38(5):1064–1068 (in Chinese).
[11] Zhou J, Yu WW, Li XM, et al. Identifying the topology of a coupled FitzHugh-Nagumo neurobiological network via a pinning mechanism. IEEE Trans Neural Netw. 2009;20(10):1679–1684.
[12] Wallace KS, Yu M, Kocarev L. Identification and monitoring of biological neural network. Proceedings of 2007 IEEE International Symposium on Circuits and systems(ISCAS); May 2007; New Orleans, USA; p. 2646–2649.
[13] Li SH, Li F, Liu WQ. Network reconstruction by linear dynamics. Physica A. 2014;404(24):118–125.
[14] Timme M. Revealing network connectivity from response dynamics. Phys Rev Lett. 2007;98(22):1–4.

[15] Yang XL, Wei T. Revealing network topology and dynamical parameters in delay-coupled complex network subjected to random noise. Nonlinear Dyn. 2015;82(1-2):319–332.
[16] Liu DF, Wu ZY, Ye QL. Structure identification of an uncertain network coupled with complex-variable chaotic systems via adaptive impulsive control. Chin Phys B. 2014;23(4):040504.
[17] Stanković MS, Stanković SS, Stipanović DM. Consensus-based decentralized real-time identification of large-scale systems. Automatica (Oxf). 2015;60:219–226.
[18] Chen L, Lu JA, Tse CK. Synchronization: an obstructer in identifying network topology based on adaptive-feedback control algorithm. IEEE Trans. Circuits Systems-II. 2009;56(4):310–314.
[19] Sun F, Peng HP, Xiao JH, et al. Identifying topology of synchronous networks by analyzing their transient processes. Nonlinear Dyn. 2012;56(4):1457–1466.
[20] Tang SX, Chen L, He YG. Optimization-based topology identification of complex networks. Chin Phys B. 2011;20(11):110502.
[21] He T, Lu XL, Wu XQ, et al. Optimization-based structure identification of dynamical networks. Physica A. 2013;392(4):1038–1049.
[22] Peng HP, Li LX, Kurths J, et al. Topology identification of complex network via chaotic ant swarm algorithm. Math Probl Eng. 2013;2013(3):401983.
[23] Van den Hof PMJ, Dankers A, Heuberger PSC, et al. Identification of dynamic models in complex networks with prediction error methods—basic methods for consistent module estimates. Automatica (Oxf). 2013;49(10):2994–3006.
[24] Ke TT. Structure identification of a sparse complex network. J Mathem. 2015;35(4):763–772.
[25] Chiuso A, Pillonetto G. A Bayesian approach to sparse network identification. Automatica (Oxf). 2012;48(8):1553–1565.
[26] Vašak M, Perić N. Combining identification and Constrained Optimal control of piecewise affine systems. Automatika. 2007;48(3–4):145–160.
[27] Hayden D, Chang YH, Goncalves J, et al. Sparse network identifiability via compressed sensing. Automatica (Oxf). 2016;68:9–17.
[28] Wang WX, Yang R, Lai Y, et al. Time-series-based prediction of complex oscillator networks via compressive sensing. Euro-physics Letters. 2011;94(4):48006.
[29] Su RQ, Wang WX, Wang X, et al. Data-based reconstruction of complex geospatial networks, nodal positioning and detection of hidden nodes. R Soc Open Sci. 2016;3(1):150577.
[30] Li GJ, Wu XQ, Liu J, et al. Recovering network topologies via Taylor expansion and compressive sensing. Chaos. 2015;25(4):043102.
[31] Zhang ZR, Niu ZS, He XZ. Synchronization of complex dynamical network with time-varying topological structure. J Lanzhou Jiaotong University. 2013;32(6):186–189 (in Chinese).
[32] Letellier C, Aguirre L. Symbolic observability coefficients for univariate and multivariate analysis. Phys Rev E. 2009;79(2):853–857.
[33] Sendiña-Nadal I, Boccaletti S, Letellier C. Observability coefficients for predicting the class of synchronizability from the algebraic structure of the local oscillators. Phys Rev E. 2016;94(4):042205.